geosciences

Article

Composition, Texture, and Weathering Controls on the Physical and Strength Properties of Selected Intrusive Igneous Rocks from Northern Pakistan

Muhammad Yasir [1], Waqas Ahmed [1], Ihtisham Islam [1,2], Muhammad Sajid [3], Hammad Tariq Janjuhah [2] and George Kontakiotis [4,*]

1 National Centre of Excellence in Geology, University of Peshawar, Peshawar 25120, Pakistan; myasir6755@uop.edu.pk (M.Y.); waqas.nce@uop.edu.pk (W.A.); ihtisham.islam@sbbu.edu.pk (I.I.)
2 Department of Geology, Shaheed Benazir Bhutto University Sheringal, Sheringal 18000, Pakistan; hammad@sbbu.edu.pk
3 Department of Geology, University of Peshawar, Peshawar 25120, Pakistan; mr.sajid@uop.edu.pk
4 Department of Historical Geology-Paleontology, Faculty of Geology and Geoenvironment, School of Earth Sciences, National and Kapodistrian University of Athens, Panepistimiopolis, Zografou, 15784 Athens, Greece
* Correspondence: gkontak@geol.uoa.gr

check for updates

Citation: Yasir, M.; Ahmed, W.; Islam, I.; Sajid, M.; Janjuhah, H.T.; Kontakiotis, G. Composition, Texture, and Weathering Controls on the Physical and Strength Properties of Selected Intrusive Igneous Rocks from Northern Pakistan. *Geosciences* **2022**, *12*, 273. https://doi.org/10.3390/geosciences12070273

Academic Editors: Michael E. Brookfield and Jesus Martinez-Frias

Received: 19 April 2022
Accepted: 4 July 2022
Published: 7 July 2022

Abstract: This study examines the mineralogy, texture, and weathering grades of intrusive igneous rocks from northern Pakistan, as well as their impacts on physical and strength properties. In comparison to felsic rocks, mafic and intermediate rocks have lower cumulative proportions of quartz, feldspar, and plagioclase, as well as higher specific gravity, strength (i.e., UCS and R-value), and UPV values. Similarly, samples with anhedral grain shapes, irregular boundaries, and fine to medium grain sizes (UD, ANS, and CGN) exhibited greater strength values, with compressive strengths of 121, 118, and 91 MPa and tensile strengths of 11, 9, and 12 MPa, respectively. The physical and strength properties of the investigated samples corresponded well with the weathering grades assigned to them, such as fresh (WG-I), slightly weathered (WG-II), and highly weathered (WG-III). That is, as the grade increased from WG-I to WG-III, the porosity and water absorption increased (0.28% and 0.72%, respectively), whereas the specific gravity, compressive strength, and tensile strength decreased (2.04, 20, and 2.5 MPa, respectively, for CGA). Although the presence of quartz impacts rock strength, no significant association was found between the strength and the maximum and mean grain sizes of other minerals.

Keywords: intrusive rocks; petrography; composition; physical properties; strength

1. Introduction

Throughout human history, rocks (whether igneous, sedimentary, or metamorphic) have been used as building materials. The strength and durability of rocks are two important factors to consider before using them as building material, dimension stones, or aggregate in concrete structures [1]. In addition to the composition, several petrographic characteristics, including modal abundance, texture, and grain size distribution, have been shown to control rock strength and stress, and strain behavior [2–4]. Weathering and alteration, on the other hand, have an impact on rock strength and durability [5–7].

The mechanical characteristics of several textural varieties of Utla granite from northwestern Pakistan were studied [8]. The substantial recrystallization and associated mineralogical changes were shown to be connected to a decrease in strength. Compressional fractures may be caused by alteration of minerals and petrological characteristics, such as exsolution in mineral phases [6]. On average, fine-grained rocks have more strength than their coarse-grained counterparts. However, when texture complexity (grain size, shape, and boundary variation) increases, so does strength [9–11]. Minerals having euhedral grains (regular boundaries) serve as discontinuities in rock structures that enable fracture formation, according to Lindqvist, Åkesson, and Malaga [10]. Other properties, such as drilling penetration resistance and thermal wear, are affected by textural variations [12]. Microtextures and fractures impact rock weathering and are principally responsible for changes in physical and mechanical properties, according to studies by Coggan, Stead, Coggan, Stead, Howe, and Faulks [6], Sajid, and Arif [8], Rigopoulos, et al. [13] and Sajid, Coggan, Arif, Andersen, and Rollinson [3]. Intense weathering and alteration in intrusive rocks may lead to the formation of secondary minerals, which include serpentine, chlorite, clay minerals, etc. [7,11,14,15]. Clay minerals have a strong capacity to absorb and then lose water, resulting in swelling and shrinkage, respectively. Because of their huge surface areas and lamellar structures, clay-bearing aggregates (when used in concrete) impair workability in general [16–18].

The Indian Plate, the Kohistan Island Arc (KIA), and the Eurasian Plate make up Pakistan's northern region [19–22]. Mansehra granite, Malakand granite, Utla granite, Ambala granite, Chakdara granite, Swat granite, and various dolerites in the form of dykes are among the intrusive igneous rocks that might be recommended as suitable building materials. The study area in the northern part of Pakistan contains a large number of ongoing civil work projects, such as hydropower complex, associated tunnels, and highways (Figure 1). There is a greater demand for new and potential aggregate sources with approachable exposures to be mined for these projects. Additionally, the characterization of the rocks is helpful in the detailed feasibility and designing of tunnels in highways and hydropower projects, such as the Basha Dam.

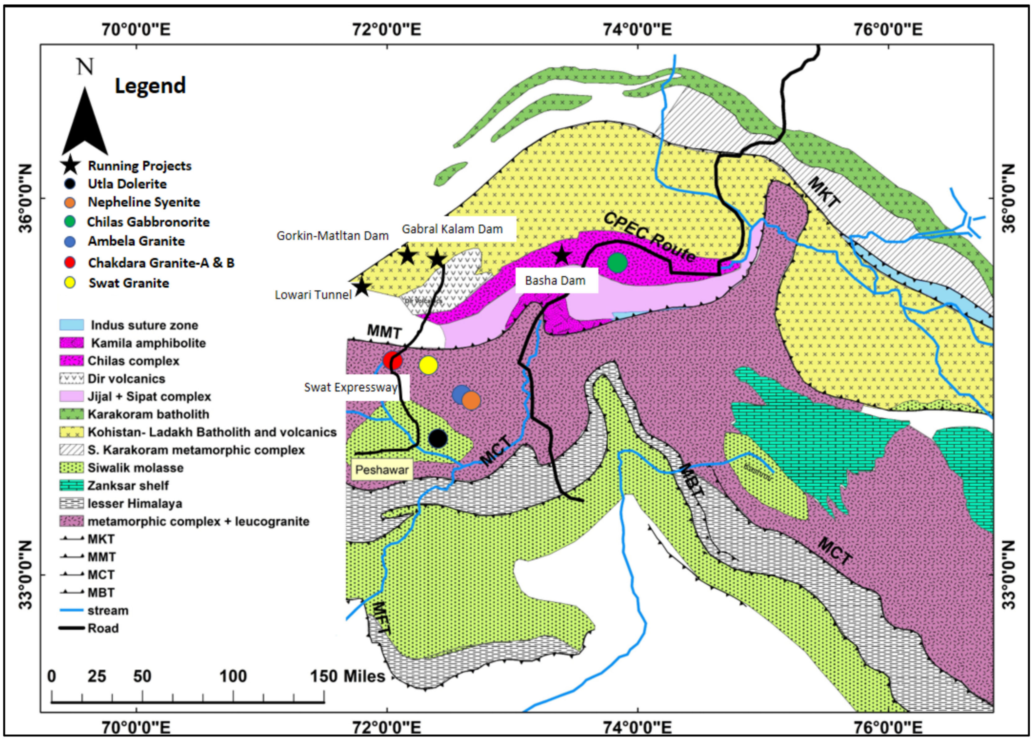

Figure 1. Geological map of northern Pakistan, modified after Searle et al. [23]. Shaded circles show the locations of the collected samples.

The effects of textural and weathering controls on mechanical behavior for a certain rock type have been thoroughly examined [3,13,23]. In contrast, this research focuses on the impacts of common textural observations gathered from numerous rock units on their mechanical characteristics. The influence of texture and weathering on the physical and strength properties of geochemically and texturally diverse intrusive rocks from northern Pakistan was examined. The rocks were primarily selected based on their access, extent, exposure, and resourcefulness. Physical testing (specific gravity, water absorption, porosity, ultrasonic pulse velocity (UPV), and strength tests (compressive, tensile, Schmidt hammer rebound(R-value) were carried out. Finally, the correlations between the petrographic and engineering attributes were statistically modeled and analyzed.

2. Geological Setting

The intra-oceanic island arc, KIA, was bounded to the north by the Eurasian plate and to the south by the Indian plate, which is separated by the Main Karakorum Thrust (MKT) and the Main Mantle Thrust (MMT), respectively (Figure 1) [19,24,25]. Starting from the south, KIA (covering an area of 36,000 km^2) mainly consists of the Jijal complex, Kamila amphibolite, Chilas complex, Gilgit gneisses, and the Chalt volcanic [26,27]. The Indian Plate consists of numerous intrusive rocks, such as Mansehra granite, Malakand granite, Utla granite, Ambela granite, Chakdara granite, Swat granite, and some dolerites in the form of dykes [2,3,28,29].

The Chilas complex, a part of KIA, represents a late cretaceous magmatic body dominantly composed of gabbronorite with a minor amount of gabbros, quartz-diorite, and tarctolites frequently intruded by the mafic dykes. The Peshawar Plain Alkaline Igneous Province (PPAIP), a part of the Indian Plate that evolved during the Permian rifting, comprises various alkaline complexes of granitic composition, including the middle to late Paleozoic Ambela granitic complex (AGC), as well as mafic dykes [30–33]. The AGC is divided into three main groups. Group-I, the first magmatic episode, includes the granite and alkali granite, which make up about 70% of the total 900 km^2 of the granitic batholith. Group-II includes syenites, nepheline syenites, quartz syenites, and feldspathoidal syenites. Group-III, the latest magmatic episode, includes mafic dykes of dolerite, metadolerite, and diorite, cross-cutting the older group-I and group-II rocks. The eastward extension of AGC, interpreted as Utla granites, is intruded by basic dykes. The petrography, geochemistry, and petrogenesis of the Utla dykes interpret its within-plate origin and suggest these dykes can be associated with the group-III rocks of the AGC [34]. The Swat-Chakdara granites are exposed in the northwestern edge of the Indian Plate, metamorphosed into Augen gneisses comprising of quartz, feldspar, muscovite, and biotite $\pm$ garnet. Anczkiewicz, et al. [35] suggested an Early Permian (276 + 40/$-$9 Ma) magmatic emplacement age for these rocks. These granites are mainly subalkaline and peraluminous and are considered to be the result of a fractional crystallization process from I-type crust granites.

3. Materials and Methods

Bulk samples of Utla dolerite (UD), Nepheline syenite (ANS), Chilas gabbronorite (CGN), Ambala granite (AG), Chakdara granite (CGB), Swat granite (SG), and Chakdara granite (CGA) were collected in the field (Figure 1). Texture, weathering grade, and mesoscopic structures were used to gather the samples (Table 1). The weathering condition (WG) was determined by examining the original texture of the rocks, as well as the color of the fresh and weathered surfaces, and the impact sound made by the geological hammer [36,37]. Weathering indicators, such as fractures, recrystallization, and mineral alteration, were also observed. Figure 2 displays cylindrical core specimens (50 mm in diameter) obtained from the investigated rock types to perform the physical and strength tests. Three core specimens from each rock sample were tested, and the average findings were reported. For the petrographic examination, thin sections were made from small slices of cores (size 40 $\times$ 20 mm). Both naked eye and microscopic observations were part of the petrographic study. Under the polarizing microscope (Eclipse LV100ND of Nikon, Tokyo, Japan), thin sections of each sample were examined. The optical characteristics of minerals were used to identify them. For textural identification, the modal abundance was estimated (based on visual estimation) and the grain shape, size, and configurations were documented [38,39].

Table 1. Details of samples collected during the fieldwork.

Rock Name	Sample Designation	Grain Size	Petrographic Description
Utla Dolerite	UD	Medium	Equigranular, euhedral to anhedral, ophitic to sub-ophitic. Plagioclase was tabular and showed a typical polysynthetic twinning. Pyroxene (mostly clinopyroxene) was subhedral to anhedral and sericitized in places.
Nepheline Syenite	ANS	Fine	Inequigranular, anhedral to euhedral grains. Alkali feldspar appeared both as perthite and microcline. Nepheline was euhedral to subhedral. Amphibole was anhedral, mostly disseminated, and altered.
Chilas Gabbronorite	CGN	Medium	Inequigranular, subhedral to anhedral grains. Plagioclase showed polysynthetic twinning and sericitization in places. Biotite was present along the margins of pyroxene grains.
Ambela Granite	AG	Coarse	Inequigranular with anhedral to subhedral grains. Alkali feldspar was perthitic, having blebs of albite. Microcline feldspar was also present. Quartz showed undulose extinction.
Chakdara Granite-B	CGB	Fine to medium	Inequigranular, anhedral to subhedral grains. Alkali feldspar was perthitic where exsolution lamellae were present and contained inclusions of mica and zircon. Quartz showed undulose extinction.
Swat Granite	SG	Medium to coarse	Inequigranular, anhedral grains. Mineral alteration and sericitization were commonly observed. Alkali feldspar contained inclusions of muscovite and quartz. Mica was mostly in tabular form and aligned.
Chakdara Granite-A	CGA	Fine to medium	Equigranular, anhedral grains. Alkali feldspar contained inclusions of mica, mostly microcline and sericitized. Quartz was mostly recrystallized. Amphibole was altered to muscovite along the margins.

The standard test methods for absorption and bulk-specific gravity of dimension stones (ASTM, DC97/C97M-18) were used to determine physical property tests, such as specific gravity and water absorption in the laboratory. The saturation technique was used to determine the porosity of the studied rocks [40]. The ultrasonic pulse velocity test device of MS CONTROLS Italy was used to estimate the UPV. A pitch–catch approach, using a pair of transducers (transmitter and receiver), was used [41]. The transit travel times of the core samples were measured at a frequency of 10 s^{-1} under two conditions: saturated surface dry (UPV_{SSD}) and oven-dry (UPV_{OD}) at 110 °C for 24 h. All tests were carried out on the same specimen, which was afterward utilized for the strength testing to achieve better correlations.

The unconfined compressive strength (UCS) test was performed using the standard test method for compressive strength and elastic moduli of intact rock core specimens under varying stresses and temperatures (ASTM, D7012-14e1). The unconfined tensile strength (UTS) test was carried out according to a Brazilian test technique for splitting the tensile strength of intact rock core specimens (ASTM, D3967-16). The Schmidt hammer rebound test (R-value) is a non-destructive way of assessing strength; it was carried out in accordance with the standard test method for the determination of rock hardness by a rebound hammer (ASTM, D5873-14). The R-value was obtained using N-type Schmidt Hammer (SH) equipment with an impact energy of 0.735 Nm.

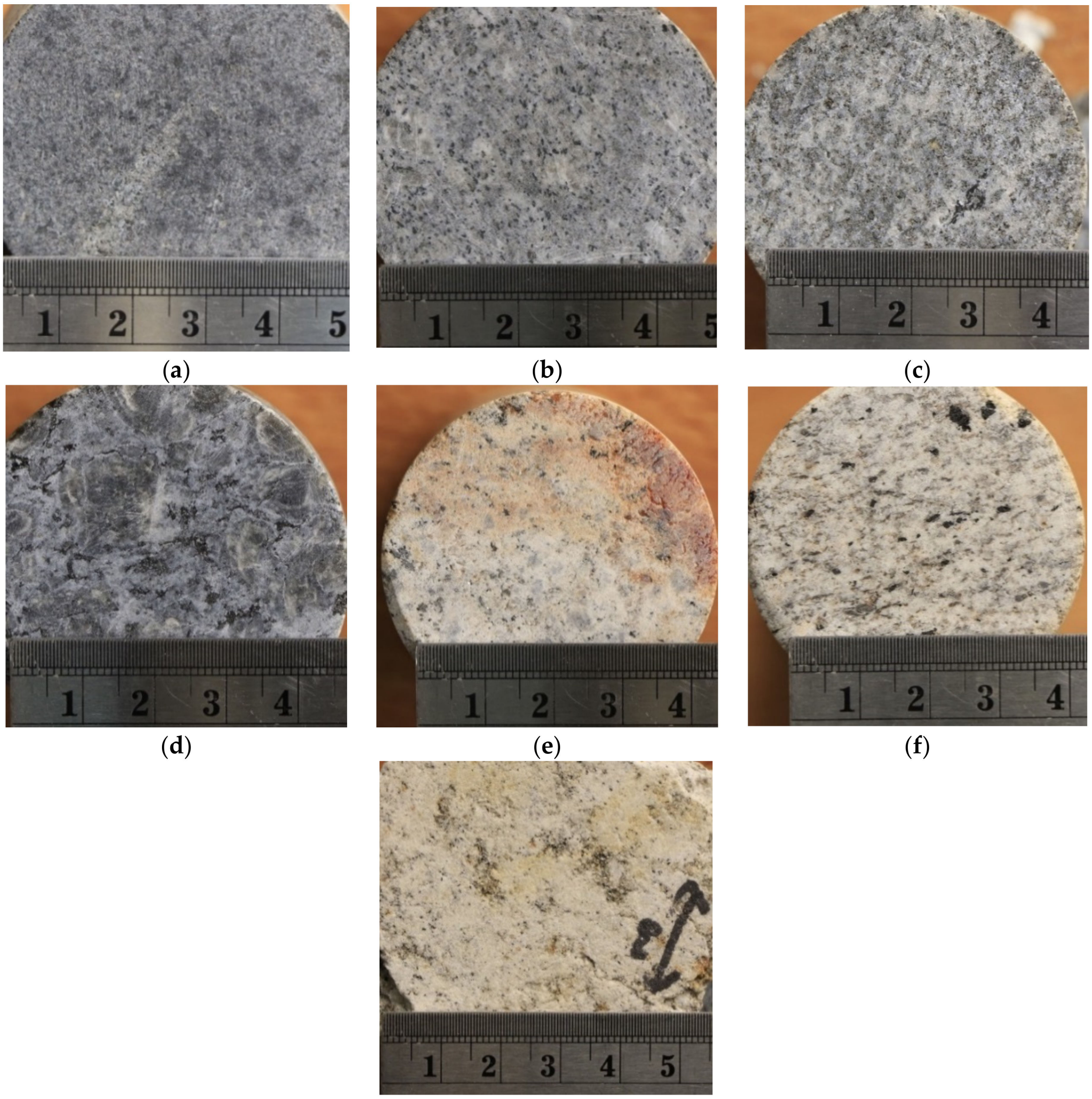

(**a**) (**b**) (**c**) (**d**) (**e**) (**f**) (**g**)

Figure 2. Photographs of the studied intrusive rocks. (**a**) Utla Dolerite (UD). (**b**) Nepheline Syenite (ANS). (**c**) Chilas Gabronorite (CGN). (**d**) Ambela Granite (AG). (**e**) Chakdara Granite-B (CGB). (**f**) Swat Granite. (**g**) Chakdara Granite-A (CGA).

4. Results and Discussion

4.1. Petrography and Weathering Grades

The chosen microphotographs of the researched rocks are shown in Figure 3, and their petrographic descriptions are included in Table 1. The modal mineralogy and mean particle sizes are shown in Table 2. The rocks are classified as mafic (UD, CGN), intermediate (ANS), or felsic (based on modal mineralogy) (AG, CGB, SG, CGA). Based on field and microscopic observations, Table 3 presents weathering grades (WG) to the examined rocks. The rocks were divided into three categories: fresh (WG-I) (UD, ANS, and CGN), slightly weathered (WG-II) (AG, CGB, and SG), and extremely weathered (WG-III) (CGA).

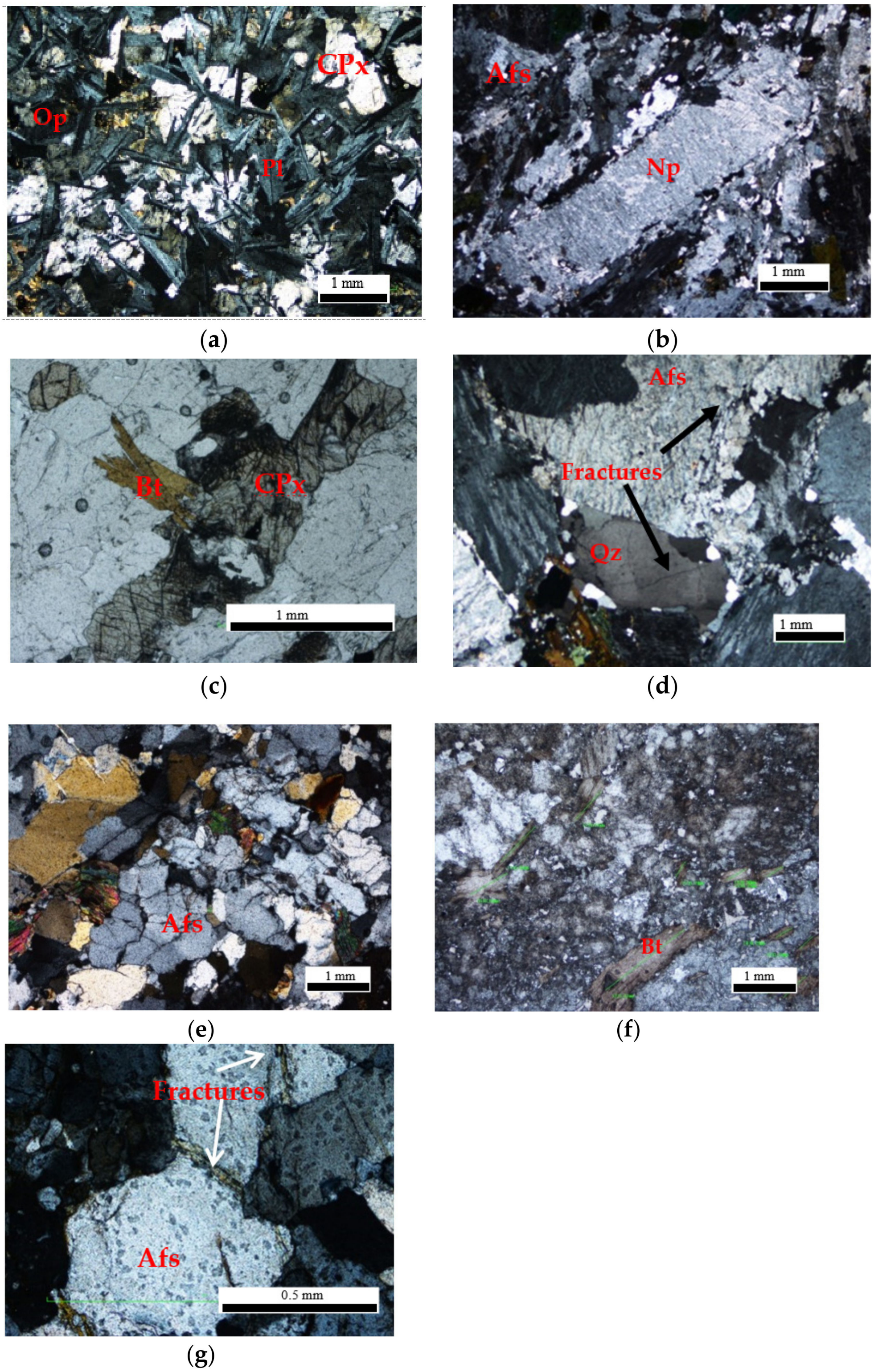

Figure 3. Microphotographs of the investigated rocks. Afs = alkali feldspar, Qz = quartz, Pl = plagioclase, Bt = biotite, Opq = opaque minerals, Nph = nepheline, CPx = clinopyroxene. (**a**) Ophitic texture of dolerite (sample UD). (**b**) Tabular phenocryst of nepheline (sample ANS). (**c**) Biotite crystallized along Cpx margins (sample CGN). (**d**) Fractures in feldspar and quartz (Sample AG). (**e**) Highly-fractured alkali feldspar and quartz (sample CGB). (**f**) Alignment of mica minerals (sample SG). (**g**) Fracture in feldspar (sample CGA).

Table 2. Modal mineralogy of the studied rocks.

Sample	Specimen	Afs	Qz	Pl	Bt	Amp	Opq	Cal	Chl	Rt	Spn	Nph	Aeg	Ap	Zrn	Ms	OPx	CPx	Ol	Grain Size * (mm)
UD	UD1	-	-	53	1	1	5	-	-	-	-	-	-	-	-	-	-	40	-	0.85
	UD2	-	-	50	1	2	8	-	-	-	-	-	-	-	-	-	-	39	-	
	UD3	-	-	51	1	2	5	-	-	-	-	-	-	-	-	-	-	41	-	
ANS	ANS1	54	-	7	T	6	-	-	-	-	4	18	11	T	T	-	-	-	-	1.07
	ANS2	56	-	7	T	4	-	-	-	-	4	21	8	T	T	-	-	-	-	
	ANS3	58	-	6	T	5	-	-	-	-	3	19	9	T	T	-	-	-	-	
CGN	CGN1	-	-	55	2	-	2	-	-	-	-	-	-	-	-	-	23	18	T	1.12
	CGN2	-	-	57	3	-	4	-	-	-	-	-	-	-	-	-	20	17	T	
	CGN3	-	-	54	2	-	5	-	-	-	-	-	-	-	-	-	21	18	T	
AG	AG1	65	13	2	9	6	2	1	-	-	-	-	-	-	-	-	-	-	-	4.15
	AG2	62	21	2	5	2	3	2	1	-	-	-	-	-	-	-	-	-	-	
	AG3	66	18	2	5	6	3	-	T	T	T	-	-	-	-	-	-	-	-	
CGB	CGB1	58	33	2	3	-	-	-	-	-	T	-	-	-	T	5	-	-	-	0.61
	CGB2	53	40	1	2	-	-	-	-	-	T	-	-	-	T	4	-	-	-	
	CGB3	56	36	3	3	-	-	-	-	-	T	-	-	-	T	4	-	-	-	
SG	SG1	34	41	8	9	4	-	-	-	-	-	-	-	-	-	4	-	-	-	1.03
	SG2	31	38	11	12	5	-	-	-	-	-	-	-	-	-	3	-	-	-	
	SG3	33	41	9	11	4	-	-	-	-	-	-	-	-	-	2	-	-	-	
CGA	CGA1	58	35	2	3	0	-	-	-	-	-	-	-	-	-	3	-	-	-	0.63
	CGA2	56	36	1	2	2	-	-	-	-	-	-	-	-	-	3	-	-	-	
	CGA3	58	34	2	3	1	-	-	-	-	-	-	-	-	-	2	-	-	-	

Afs = alkali feldspar, Qz = quartz, Pl = plagioclase, Bt = biotite, Amp = amphibole, Opq = opaque minerals, Cal = calcite, RT = rutile and Spn = sphene, Nph = nepheline, Aeg = aegirine, Ap = apatite and Zrn = zircon, Ms = muscovite, CPx = clinopyroxene, T = trace, * mean grain size (mm) (mineral abbreviations are according to Whitney and Evans, 2010).

Table 3. Weathering classification of the investigated rocks (after Irfan and Dearman [37] and Borrelli, Greco, and Gullà [36].

Sample	Outcrop Observations	Microscopic Observations	Descriptive Term	Weathering GRADE
UD	Dark grey to black in color, uniform and fine-grained. Very compact and produced a sharp sound with a geological hammer.	Ophitic to sub-ophitic texture, with polysynthetic twinning in plagioclase, was mostly fresh but slight alteration was observed in pyroxene.	Fresh	I
ANS	Fine to medium-grained, grey, and no discoloration. Purely fresh and produced a good sharp sound with a geologic hammer.	Major minerals, such as feldspar and nepheline, were fresh, but a slight alteration of amphibole was observed.	Fresh	I
CGN	Greyish in color on fresh, while brown on the weathered surface, medium-grained. Very hard, having compact sound with a geologic hammer.	A slight alteration was observed in plagioclase and pyroxene at places, but overall, dominantly consisted of fresh mineral grains.	Fresh	I
AG	Milky white color with dark greyish phenocryst, medium-grained, original texture was preserved. Produced a compact sound when struck with a geological hammer. The weathered surface color was brownish-grey.	Minerals with a fresh appearance and no signs of prominent alteration. Some fractures in feldspar and quartz were present.	Slightly weathered	II
CGB	Light brown, fine to medium-grained. Slight discoloration and moderately foliated. Fairly compact sound with a geologic hammer.	Comparatively fresh mineral grains to CGA; however, alteration of feldspar was observed.	Slightly weathered	II
SG	White in color, moderately gneissose, and medium to coarse-grained. Slightly fresh and produced a dull sound with a geological hammer.	Alteration and sericitization were observed in both feldspar and micas. Feldspar was fractured and mica was mostly aligned.	Slightly weathered	II
CGA	Milky white in color, fine-grained, having discoloration. Extremely sheared and foliated. Produced a dull sound and was easily breakable with a geologic hammer.	The thin section appearance was dirty. Major minerals, such as feldspar and quartz, were highly fractured. Sericitization and alteration were commonly observed in feldspar and amphibole.	Highly weathered	III

AG = Ambela granite, ANS = Nepheline syenite, CGA = Chakdara granite A, CGB = Chakdara Granite B, CGN = Chilas gabbronorite, SG = Swat granite, UD = Utla dolerite.

4.2. Physical Properties

The average findings for physical attributes are shown in Table 4. Fresh WG-I samples (UD, ANS, and CGN) had greater specific gravity and UPV_{sat} (3.08 and 5573.17 m/s for UD, respectively), but lower WA (0.13% for CGN), and porosity (0.12% for ANS). WG-III (CGA), a highly weathered sample, had the lowest specific gravity (2.04) and UPV_{dry} (1526.26 m/s), as well as the highest water absorption (WA) (0.28%) and porosity (0.72%). UPV findings showed a slight decrease from UPV_{sat} to UPV_{dry}, except for CGA, which showed a slight rise. These findings support previous research on the effects of weathering on granites, which found that a material with a high porosity may hold more water, resulting in lower UPV values [42,43].

Table 4. Results of physical and strength properties of the investigated rocks.

Sample	Specimen	Specific Gravity	Water Absorption (%)	Porosity (%)	UPV_{Sat} (m/s)	UPV_{OD} (m/s)	UCS (MPa)	UTS (MPa)	R-Value
UD	UD 1	3.08	0.16	0.37	5784.71	5421.05	121.07	10.1	53.67
	UD 2	3.07	0.17	0.39	5527.52	5095.14	122.7	10.8	54.33
	UD 3	3.08	0.14	0.36	5407.24	4910.96	118.33	10.6	53.33
ANS	ANS 1	2.69	0.19	0.12	3185.92	3496.14	115.86	12	46.67
	ANS 2	2.68	0.18	0.11	4776.92	3722.28	120.27	7.7	48.33
	ANS 3	2.68	0.20	0.13	4673.6	3671.09	118.07	8.3	47.33
CGN	CGN 1	2.92	0.20	0.29	4096.81	4617.46	95.97	11	45.33
	CGN 2	2.92	0.10	0.28	4915.9	4629.95	86.7	13.8	43.67
	CGN 3	2.92	0.09	0.27	5295.18	4428.21	91.37	12.4	44.00
AG	AG 1	2.68	0.06	0.17	2806.03	2580.41	65.24	6.8	33.00
	AG 2	2.67	0.05	0.14	2682.35	2480.96	66.79	5.5	39.00
	AG 3	2.66	0.07	0.12	3199.77	2329.5	47.8	5.8	34.33
CGB	CGB 1	2.63	0.17	0.44	2349.17	2656.54	53.31	6.5	20.67
	CGB 2	2.64	0.18	0.46	2321.39	2559.82	53.84	5.6	22.33
	CGB 3	2.64	0.16	0.42	2410.49	2606.53	52.79	6.1	20.33
SG	SG 1	2.67	0.17	0.28	3505.29	2486.01	41.49	5.3	32.67
	SG 2	2.67	0.09	0.25	2818.04	2559.32	48.55	5.9	33.67
	SG 3	2.59	0.10	0.26	3304.51	2316.64	45.01	5.6	32.00
CGA	CGA 1	2.07	0.26	0.72	1500	1949.22	23.62	2.4	14.00
	CGA 2	2.06	0.28	0.71	1449.74	1684.13	19.98	2.6	13.67
	CGA 3	2	0.29	0.74	1072.93	945.42	17.7	2.5	13.33

4.3. Strength Properties

The tested rocks' strength values corresponded to their physical characteristics (Table 4), i.e., fresh, WG-I samples had greater UCS (120 MPa for UD) and UTS values (12.40 MPa for CGN). Whereas the highly weathered, WG-III showed lower UCS and UTS values (20 MPa and 2.5 MPa, respectively, for CGA). Previous research from Pakistan and other regions of the globe produced similar findings [2,5,8,44,45]. Similarly, fresh WG-I samples had a high R-value (53.78 for UD) while highly-weathered WG-III samples had the lowest (13.67 for CGA).

4.4. Petrographic, Physical, and Strength Properties

The researched rock types' petrographic, physical, and strength properties are addressed.

- Sample UD had a significant percentage of opaque minerals (5% to 8%), which led to a higher specific gravity (3.08). The greater porosity (0.37%) was also attributable to slight pyroxene mineral alteration (Figure 3a) and intergranular fractures. Fresh WG-I samples and UD had the greatest UCS and UTS values among the studied samples (121 and 11 MPa, respectively).

- The alkali feldspar and amphibole in the ANS sample were slightly altered, resulting in relatively high water absorption and porosity values (0.19% and 0.12%, respectively). It did, however, have high UCS and UTS values (118 MPa and 9 MPa, respectively), as well as a fresh weathering grade (WG-I). The higher strengths are attributed to the inequigranular, anhedral grains, and irregular boundaries, mainly of fine-grained feldspar surrounding the tabular nepheline (Figure 3b).
- The grain size of the sample CGN was uniform, and the boundaries were regular. When compared to other fresh, WG-I samples, the twinning and slight alteration of plagioclase (Figure 3c) resulted in moderate water absorption and porosity (i.e., 0.13% and 0.28%, respectively), as well as reduced UCS and UTS values (i.e., 91 MPa and 12 MPa, respectively).
- Among the studied samples, sample AG had the lowest water absorption and porosity (0.06% and 0.14%, respectively). Its moderate UCS and UTS values (60 MPa and 6 MPa, respectively) and slightly weathered, WG-II weathering grade were due to its subhedral grain shape and the presence of large feldspar grains (up to 10 mm) with intra-granular fractures (Figure 3d).
- The sample CGB had more fresh alkali feldspar, quartz, and mica grains than CGA (Figure 3e), resulting in lower water absorption and porosity (0.17% and 0.44%, respectively), greater UCS and UTS values (53 MPa and 6 MPa, respectively), and a slightly weathered WG-II weathering-grade.
- Gneissosity was seen in the form of aligned flaky mica in the sample SG (Figure 3f). Furthermore, it exhibited gneissosity and moderate weathering (WG-II), resulting in modest water absorption and porosity (0.12% and 0.26%, respectively). UCS and UTS values were affected by sericitization and fractures of Alkali feldspar (i.e., 45 MPa and 6 MPa, respectively). Similar observations were reported by Åkesson [46] on microstructures in Swedish granites and marbles.
- The CGA sample was substantially sheared (WG-III), with sericitization, alteration, and extensive fracturing of alkali feldspar (Figure 3g). As a consequence, substantial levels of water absorption and porosity were achieved (0.28% and 0.62%, respectively). It had the lowest UCS and UTS values of all the samples studied (20 MPa and 3 MPa, respectively).

Figure 4 depicts the regression analysis used to study the influence of mineralogy and weathering grades on the physical and strength properties of the analyzed rocks. Inverse correlations are found (Figure 4a–e) when the cumulative proportion of quartz, feldspar, and plagioclase (Q + F + P) are plotted against specific gravity, UCS, R-value, and UPV, with R^2 = 0.62, 0.81, 0.90, and 0.90, respectively. Figure 4a demonstrates that mafic and intermediate rocks with lower cumulative percentages of Q + F + P have greater specific gravity than fresh rocks (WG-I) with higher cumulative percentages of Q + F + P. (2.68 to 3.08). The felsic rocks, which range from slightly weathered to highly weathered (WG-II and WG-III) and had higher cumulative proportions of Q + F + P, have a lower specific gravity (2.0 to 2.67). Rocks with a greater specific gravity indicate the presence of heavy and high-strength minerals, which have a considerable influence on the strength of the rock (Figure 4d). These results are consistent with those of Sajid, Coggan, Arif, Andersen, and Rollinson [3], who compared the modal compositions of quartz, plagioclase, and feldspar to the UCS, finding negative correlations for quartz and plagioclase, but positive correlations for feldspar. Similarly, mafic rocks have higher UPV_{OD} values (Figure 4e) with R^2 = 0.90 when compared to felsic rocks, as reported by Behn and Kelemen [47].

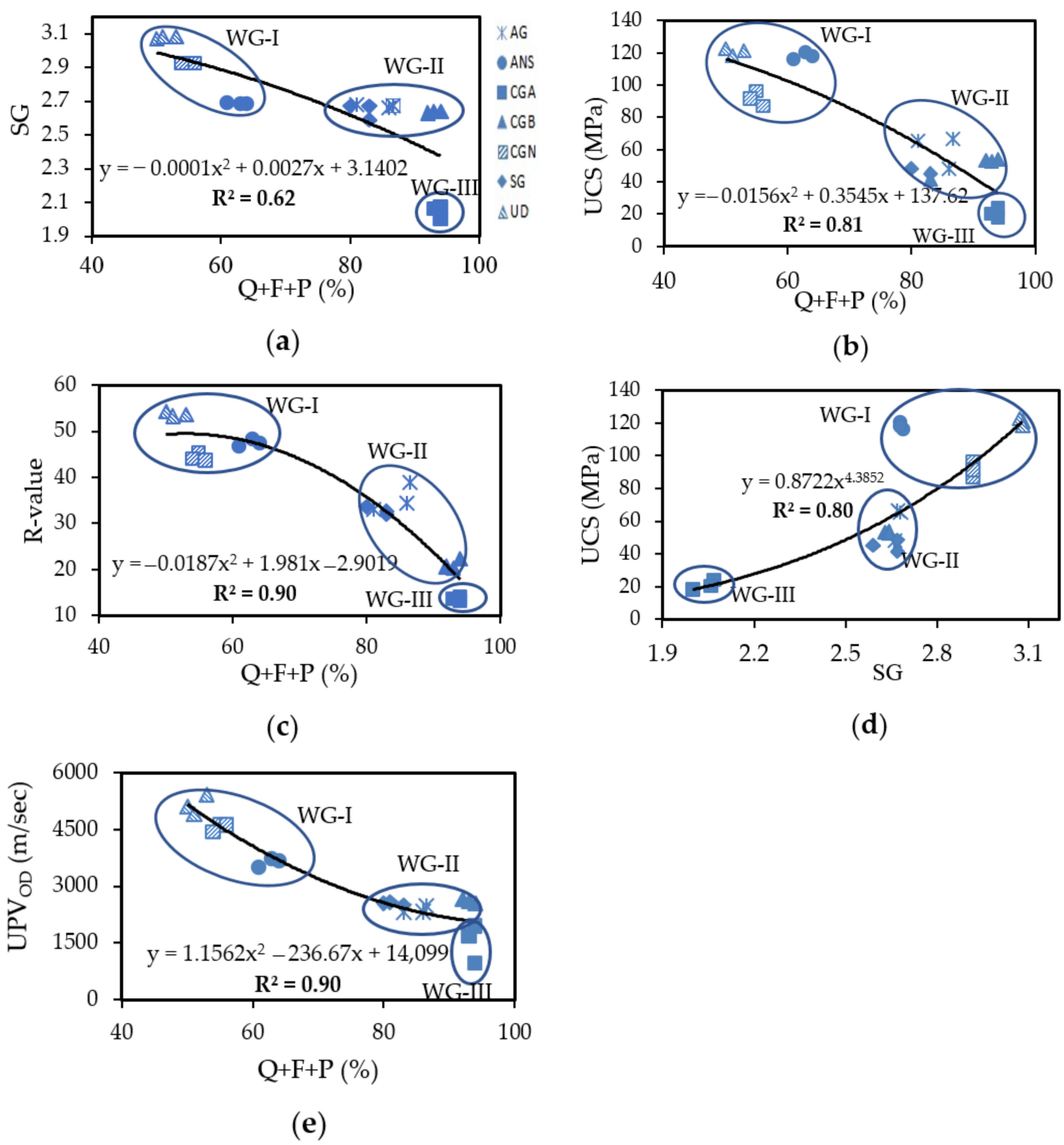

Figure 4. Correlation plots of (**a**) cumulative percentage of quartz, feldspar, and plagioclase (Q + F + P) vs. specific gravity (SG) (polynomial), (**b**) Q + F + P vs. unconfined compressive strength (UCS) (polynomial), (**c**) UCS vs. SG, (**d**) Q + F + P vs. R-value (polynomial), (**e**) Q + F + P vs. ultrasonic pulse velocity oven-dry (UPV OD) (polynomial). Symbols given in (**a**) are the same for all figures.

Aldeeky and Al Hattamleh [48], Ercikdi, et al. [49], Gomez-Heras, et al. [50], Selçuk and Nar [51], and Yılmaz, et al. [52] stated that using UPV and thorough petrography could evaluate the fractures and compactness of rocks. Yılmaz, Ercikdi, Karaman, and Külekçi [52] found a link between specific gravity and UPV, demonstrating that compact rocks had higher UPV values. With R^2 = 0.89, Figure 5a shows UPV and specific gravity. The compressional waves of UPV provide varied outcomes for different pore-filled fluids in the rocks, with UPV_{OD} and UPV_{SSD} showing a usually positive correlation [53–55]. Figure 5b reveals that UPV_{OD} and UPV_{SSD} have a positive connection (R^2 = 0.87). Figure 5c,d indicate substantial positive associations between UPV_{OD} and UCS and the R-value (R^2 = 0.85 and R^2 = 0.82, respectively). These findings are consistent with those by Vasconcelos, Lourenco, Alves, and Pamplona [43], Vasanelli, Sileo, Calia, and Aiello [55], and Akoglu, et al. [56]. The R-value and UCS have a positive association (R^2 = 0.89), as shown in Figure 5e.

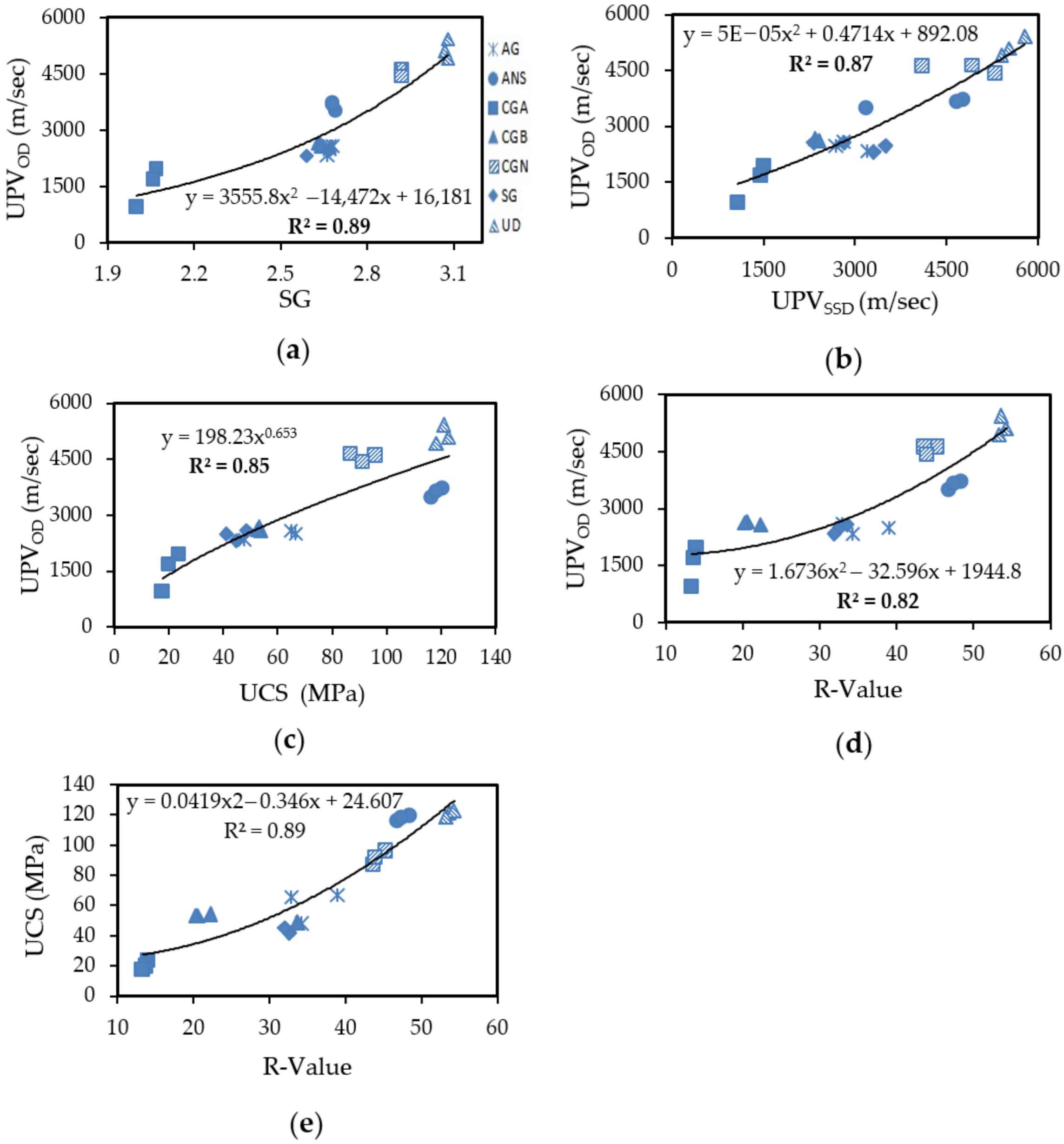

Figure 5. Correlation plots of (**a**) ultrasonic pulse velocity oven-dry (UPV_{OD}) vs. specific gravity (SG) (polynomial), (**b**) UPV_{OD} vs. UPV_{SSD} (polynomial), (**c**) UPV_{OD} vs. UCS (power) (**d**) UPV_{OD} vs. R-Value (polynomial), (**e**) UPV_{OD} vs. R-Value (polynomial). Symbols given in (**a**) are the same for all figures.

The effects of modal composition, weathering grade, and grain size on the rock strength are shown in Figure 6. The rock strength reduces as the weathering grade increases from WG-I to WG-III and the composition changes from mafic to felsic (Figure 6a). The presence of quartz affects the rock strength, which is consistent with previous research. In contrast to earlier research by Sajid and Arif [8] and Tuğrul [5], and others, no significant correlation was found when the rock strength was plotted against maximum and mean grain sizes of various minerals (Figure 6b,c). This shows that weathering has a dominant effect on the rock strength irrespective of the grain size. To achieve any meaningful relationship between the grain size effect of a particular mineral or overall grain size on the rock strength, rocks with similar weathering grades must be considered.

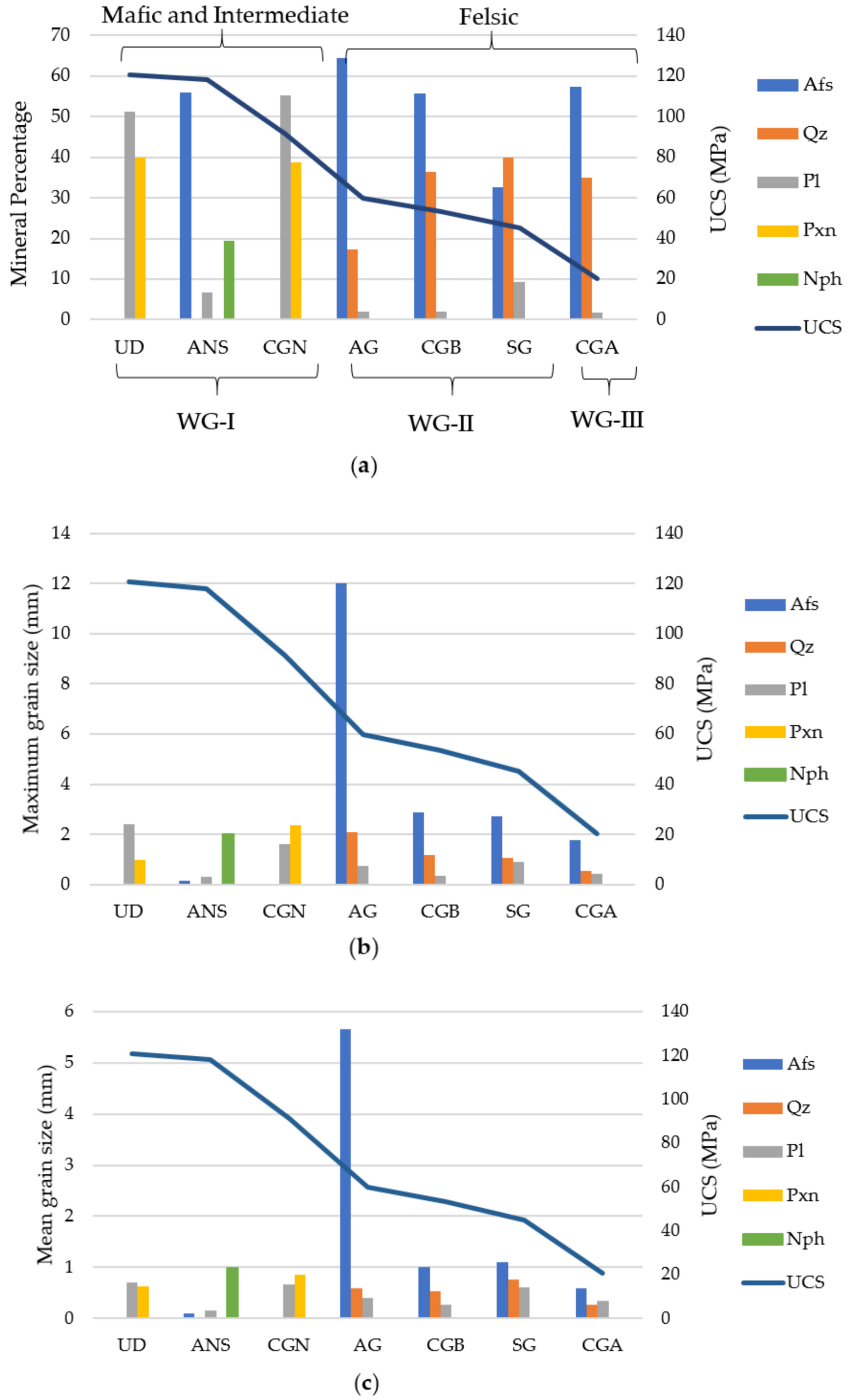

Figure 6. Relationship between the petrographic characteristics, weathering grade, and strength. (**a**) Effect of mineral composition and weathering grades on the strengths of mafic, intermediate, and felsic rocks. (**b**) Effects of maximum grain sizes of minerals and weathering grades on the strengths of mafic, intermediate, and felsic rocks. (**c**) Effects of mean grain sizes of minerals and weathering grades on the strengths of mafic, intermediate, and felsic rocks.

5. Conclusions

This research presents the results of field and petrographic observations, and physical and strength parameters of selected intrusive rocks from northern Pakistan. The examined intrusive igneous rocks were classified as fresh, WG-I (UD, ANS, and CGN), slightly weathered, WG-II (AG, CGB, and SG), and highly weathered, WG-III(CGA), based on detailed laboratory testing. Weathering grades were shown to have a strong relationship with physical and strength properties. Fresh WG-I samples (UD, ANS, and CGN) had greater specific gravity and UPV_{sat} (3.08 and 5573.17 m/s for UD, respectively), but lower WA (0.13% for CGN) and porosity (0.12% for ANS). WG-III (CGA), a heavily weathered sample, had the lowest specific gravity (2.04) and UPV_{OD} (1526.26 m/s), as well as the highest water absorption (WA) (0.28%) and porosity (0.72%). Fresh WG-I samples had higher UCS (120 MPa for UD) and UTS values as well (12.40 MPa for CGN). The WG-III sample had lower UCS and UTS values while being heavily weathered (20 MPa and 2.5 MPa, respectively, for CGA). In comparison to UPV_{SSD}, the ultrasonic pulse velocity of UPV_{OD} was slightly lower. As the composition of rocks changed from mafic to felsic, the rock's strength decreased. Although the presence of quartz impacts rock strength, no significant link was found between rock strength and the maximum and mean grain sizes of other minerals. From the findings, it may be concluded that previous researchers' correlations cannot be generalized to any other rock type.

Author Contributions: Conceptualization, W.A. and M.Y.; methodology, M.Y. and W.A.; software, M.Y.; validation, W.A., M.Y., I.I. and M.S.; formal analysis, M.Y.; investigation, W.A., M.Y., I.I., M.S., H.T.J. and G.K.; resources, M.Y.; data curation, W.A. and M.Y.; writing—original draft preparation, M.Y. and W.A.; writing—review and editing, W.A., M.Y., I.I., M.S., H.T.J. and G.K.; visualization, W.A., M.Y., I.I., H.T.J. and G.K.; supervision, W.A.; funding acquisition, G.K. All authors have read and agreed to the published version of the manuscript.

Funding: This research received no external funding.

Institutional Review Board Statement: Not applicable.

Informed Consent Statement: Not applicable.

Data Availability Statement: The data used in this work are available upon request.

Acknowledgments: The authors would like to thank the National Centre of Excellence in Geology, University of Peshawar, for providing funding for the fieldwork and laboratory facilities. The authors also thank Muhammad Hamad for digitizing the geological map of the study area.

Conflicts of Interest: The authors declare no conflict of interest.

References

1. Petrounias, P.; Giannakopoulou, P.P.; Rogkala, A.; Stamatis, P.M.; Lampropoulou, P.; Tsikouras, B.; Hatzipanagiotou, K. The effect of petrographic characteristics and physico-mechanical properties of aggregates on the quality of concrete. *Minerals* **2018**, *8*, 577. [CrossRef]
2. Arif, M.; Mulk, A.; Tariq, M.; Majid, S. Petrography and mechanical properties of the Mansehra granite, Hazara, Pakistan. *Geol. Bull. Univ. Peshawar* **1999**, *32*, 41–49.
3. Sajid, M.; Coggan, J.; Arif, M.; Andersen, J.; Rollinson, G. Petrographic features as an effective indicator for the variation in strength of granites. *Eng. Geol.* **2016**, *202*, 44–54. [CrossRef]
4. Sousa, L.M. The influence of the characteristics of quartz and mineral deterioration on the strength of granitic dimensional stones. *Environ. Earth Sci.* **2013**, *69*, 1333–1346. [CrossRef]
5. Tuğrul, A. The effect of weathering on pore geometry and compressive strength of selected rock types from Turkey. *Eng. Geol.* **2004**, *75*, 215–227. [CrossRef]
6. Coggan, J.; Stead, D.; Howe, J.; Faulks, C. Mineralogical controls on the engineering behavior of hydrothermally altered granites under uniaxial compression. *Eng. Geol.* **2013**, *160*, 89–102. [CrossRef]
7. Petrounias, P.; Rogkala, A.; Kalpogiannaki, M.; Tsikouras, B.; Hatzipanagiotou, K. Comparative study of physicomechanical properties of ultrabasic rocks and andesites from central macedonia (Greece). *Bull. Geol. Soc. Greece* **2016**, *50*, 1989–1998. [CrossRef]
8. Sajid, M.; Arif, M. Reliance of physico-mechanical properties on petrographic characteristics: Consequences from the study of Utla granites, north-west Pakistan. *Bull. Eng. Geol. Environ.* **2015**, *74*, 1321–1330. [CrossRef]

9. Åkesson, U.; Stigh, J.; Lindqvist, J.E.; Göransson, M. The influence of foliation on the fragility of granitic rocks, image analysis and quantitative microscopy. *Eng. Geol.* **2003**, *68*, 275–288. [CrossRef]
10. Lindqvist, J.-E.; Åkesson, U.; Malaga, K. Microstructure and functional properties of rock materials. *Mater. Charact.* **2007**, *58*, 1183–1188. [CrossRef]
11. Tuğrul, A.; Zarif, I. Correlation of mineralogical and textural characteristics with engineering properties of selected granitic rocks from Turkey. *Eng. Geol.* **1999**, *51*, 303–317. [CrossRef]
12. Howarth, D.F.; Rowlands, J.C. Development of an index to quantify rock texture for qualitative assessment of intact rock properties. *Geotech. Test. J.* **1986**, *9*, 169–179.
13. Rigopoulos, I.; Tsikouras, B.; Pomonis, P.; Hatzipanagiotou, K. The influence of alteration on the engineering properties of dolerites: The examples from the Pindos and Vourinos ophiolites (Northern Greece). *Int. J. Rock Mech. Min. Sci.* **2010**, *47*, 69–80. [CrossRef]
14. Petrounias, P.; Giannakopoulou, P.P.; Rogkala, A.; Lampropoulou, P.; Koutsopoulou, E.; Papoulis, D.; Tsikouras, B.; Hatzipanagiotou, K. The Impact of Secondary Phyllosilicate Minerals on the Engineering Properties of Various Igneous Aggregates from Greece. *Minerals* **2018**, *8*, 329. [CrossRef]
15. Shakoor, A.; Bonelli, R.E. Relationship between petrographic characteristics, engineering index properties, and mechanical properties of selected sandstones. *Bull. Assoc. Eng. Geol.* **1991**, *28*, 55–71. [CrossRef]
16. Bish, D.L.; Howard, S. Quantitative phase analysis using the Rietveld method. *J. Appl. Crystallogr.* **1988**, *21*, 86–91. [CrossRef]
17. Petrounias, P.; Giannakopoulou, P.P.; Rogkala, A.; Stamatis, P.M.; Tsikouras, B.; Papoulis, D.; Lampropoulou, P.; Hatzipanagiotou, K. The Influence of Alteration of Aggregates on the Quality of the Concrete: A Case Study from Serpentinites and Andesites from Central Macedonia (North Greece). *Geosciences* **2018**, *8*, 115. [CrossRef]
18. Tiwari, B.; Ajmera, B. Consolidation and swelling behavior of major clay minerals and their mixtures. *Appl. Clay Sci.* **2011**, *54*, 264–273. [CrossRef]
19. Coward, M.P.; Rex, D.C.; Khan, M.A.; Windley, B.F.; Broughton, R.D.; Luff, I.W.; Petterson, M.G.; Pudsey, C.J. Collision tectonics in the NW Himalayas. *Geol. Soc. Lond. Spec. Publ.* **1986**, *19*, 203–219. [CrossRef]
20. Tahirkheli, R.K. The India-Eurasia suture zone in northern Pakistan: Synthesis and interpretation of recent data at plate scale. *Geodyn. Pak.* **1979**, 125–130.
21. Ishfaque, M.; Dai, Q.; Haq, N.u.; Jadoon, K.; Shahzad, S.M.; Janjuhah, H.T. Use of Recurrent Neural Network with Long Short-Term Memory for Seepage Prediction at Tarbela Dam, KP, Pakistan. *Energies* **2022**, *15*, 3123. [CrossRef]
22. Khan, J.; Ahmed, W.; Yasir, M.; Islam, I.; Janjuhah, H.T.; Kontakiotis, G. Pollutants Concentration during the Construction and Operation Stages of a Long Tunnel: A Case Study of Lowari Tunnel, (Dir–Chitral), Khyber Pakhtunkhwa, Pakistan. *Appl. Sci.* **2022**, *12*, 6170. [CrossRef]
23. Searle, M.; Khan, M.A.; Fraser, J.; Gough, S.; Jan, M.Q. The tectonic evolution of the Kohistan-Karakoram collision belt along the Karakoram Highway transect, north Pakistan. *Tectonics* **1999**, *18*, 929–949. [CrossRef]
24. Jan, M.Q. Geochemistry of amphibolites from the southern part of the Kohistan arc, N. Pakistan. *Mineral. Mag.* **1988**, *52*, 147–159. [CrossRef]
25. TAHIRKHELI, R.K. Geology of kohistan, karakoram, himalaya, northern. *Geol. Bull. Univ. Peshawar* **1979**, *11*, 1–30.
26. Burg, J.; Bodinier, J.; Chaudhry, S.; Hussain, S.; Dawood, H. Infra-arc mantle-crust transition and intra-arc mantle diapirs in the Kohistan Complex (Pakistani Himalaya): Petro-structural evidence. *Terra Nova-Oxf.* **1998**, *10*, 74–80. [CrossRef]
27. Khan, M.A.; Treloar, P.J.; Khan, M.A.; Khan, T.; Qazi, M.S.; Jan, M.Q. Geology of the Chalt–Babusar transect, Kohistan terrane, N. Pakistan: Implications for the constitution and thickening of island-arc crust. *J. Asian Earth Sci.* **1998**, *16*, 253–268. [CrossRef]
28. Din, F.; Rafiq, M. Correlation between compressive strength and tensile strength/index strength of some rocks of North-West Frontier Province (limestone and granite). *Geol. Bull. Univ. Peshawar* **1997**, *30*, 183.
29. Janjuhah, H.T.; Ishfaque, M.; Mehmood, M.I.; Kontakiotis, G.; Shahzad, S.M.; Zarkogiannis, S.D. Integrated Underground Mining Hazard Assessment, Management, Environmental Monitoring, and Policy Control in Pakistan. *Sustainability* **2021**, *13*, 13505. [CrossRef]
30. Kempe, D. The petrology of the Warsak alkaline granites, Pakistan, and their relationship to other alkaline rocks of the region. *Geol. Mag.* **1973**, *110*, 385–404. [CrossRef]
31. Kempe, D.R.C.; Jan, M.Q. The Peshawar Plain Alkaline Igneous Province. NW Pakistan. *Geol. Bull. Univ. Peshawar* **1980**, *13*, 71–77.
32. Ali, S.K.; Janjuhah, H.T.; Shahzad, S.M.; Kontakiotis, G.; Saleem, M.H.; Khan, U.; Zarkogiannis, S.D.; Makri, P.; Antonarakou, A. Depositional Sedimentary Facies, Stratigraphic Control, Paleoecological Constraints, and Paleogeographic Reconstruction of Late Permian Chhidru Formation (Western Salt Range, Pakistan). *J. Mar. Sci. Eng.* **2021**, *9*, 1372. [CrossRef]
33. Bilal, A.; Mughal, M.S.; Janjuhah, H.T.; Ali, J.; Niaz, A.; Kontakiotis, G.; Antonarakou, A.; Usman, M.; Hussain, S.A.; Yang, R. Petrography and Provenance of the Sub-Himalayan Kuldana Formation: Implications for Tectonic Setting and Palaeoclimatic Conditions. *Minerals* **2022**, *12*, 794. [CrossRef]
34. Majid, M.; Danishwar, S.; Hamidullah, S. Petrographic and chemical variations in the rift-related basic dykes of the Malka Area (Lower Swat), NWFP, Pakistan. *Geol. Bull. Univ. Peshawar* **1991**, *24*, 1–23.
35. Anczkiewicz, R.; Burg, J.-P.; Hussain, S.; Dawood, H.; Ghazanfar, M.; Chaudhry, M. Stratigraphy and structure of the Indus Suture in the lower Swat, Pakistan, NW Himalaya. *J. Asian Earth Sci.* **1998**, *16*, 225–238. [CrossRef]

36. Borrelli, L.; Greco, R.; Gullà, G. Weathering grade of rock masses as a predisposing factor to slope instabilities: Reconnaissance and control procedures. *Geomorphology* **2007**, *87*, 158–175. [CrossRef]
37. Irfan, T.Y.; Dearman, W.R. Engineering Classification and Index Properties of a Weathered Granite. *Bull. Int. Assoc. Eng. Geol. Bull. Assoc. Int. Géologie Ingénieur* **1978**, *17*, 79–90.
38. Janjuhah, H.T.; Sanjuan, J.; Alquadah, M.; Salah, M.K. Biostratigraphy, Depositional and Diagenetic Processes in Carbonate Rocks form Southern Lebanon: Impact on Porosity and Permeability. *Acta Geol. Sin.-Engl. Ed.* **2021**, *5*, 1668–1683. [CrossRef]
39. Janjuhah, H.T.; Kontakiotis, G.; Wahid, A.; Khan, D.M.; Zarkogiannis, S.D.; Antonarakou, A. Integrated Porosity Classification and Quantification Scheme for Enhanced Carbonate Reservoir Quality: Implications from the Miocene Malaysian Carbonates. *J. Mar. Sci. Eng.* **2021**, *9*, 1410. [CrossRef]
40. Franklin, J.A. Suggest methods for determining water content, porosity, density, absorption and related properties and swelling and slake-durability index properties. *Int. J. Rock Mech. Min. Sci. Geomech.* **1979**, *16*, 141–156.
41. Aydin, A. Upgraded ISRM suggested method for determining sound velocity by ultrasonic pulse transmission technique. In *The ISRM Suggested Methods for Rock Characterization, Testing and Monitoring: 2007–2014*; Springer: Berlin/Heidelberg, Germany, 2013; pp. 95–99.
42. Sousa, L.M.; del Rio, L.M.S.; Calleja, L.; de Argandona, V.G.R.; Rey, A.R. Influence of microfractures and porosity on the physico-mechanical properties and weathering of ornamental granites. *Eng. Geol.* **2005**, *77*, 153–168. [CrossRef]
43. Vasconcelos, G.; Lourenco, P.B.; Alves, C.A.; Pamplona, J. Ultrasonic evaluation of the physical and mechanical properties of granites. *Ultrasonics* **2008**, *48*, 453–466. [CrossRef] [PubMed]
44. Rafique, A.; Burian, S.; Hassan, D.; Bano, R. Analysis of Operational Changes of Tarbela Reservoir to Improve the Water Supply, Hydropower Generation, and Flood Control Objectives. *Sustainability* **2020**, *12*, 7822. [CrossRef]
45. Basu, A.; Celestino, T.; Bortolucci, A. Evaluation of rock mechanical behaviors under uniaxial compression with reference to assessed weathering grades. *Rock Mech. Rock Eng.* **2009**, *42*, 73–93. [CrossRef]
46. Åkesson, U. Microstructures in Granites and Marbles in Relation to Their Durability as a Construction Material. Ph.D. Thesis, University of Gothenburg, Gothenburg, Sweden, 2004.
47. Behn, M.D.; Kelemen, P.B. Relationship between seismic P-wave velocity and the composition of anhydrous igneous and meta-igneous rocks. *Geochem. Geophys. Geosyst.* **2003**, *4*, 1–57. [CrossRef]
48. Aldeeky, H.; Al Hattamleh, O. Prediction of engineering properties of basalt rock in Jordan using ultrasonic pulse velocity test. *Geotech. Geol. Eng.* **2018**, *36*, 3511–3525. [CrossRef]
49. Ercikdi, B.; Karaman, K.; Cihangir, F.; Yılmaz, T.; Aliyazıcıoğlu, Ş.; Kesimal, A. Core size effect on the dry and saturated ultrasonic pulse velocity of limestone samples. *Ultrasonics* **2016**, *72*, 143–149. [CrossRef]
50. Gomez-Heras, M.; Benavente, D.; Pla, C.; Martinez-Martinez, J.; Fort, R.; Brotons, V. Ultrasonic pulse velocity as a way of improving uniaxial compressive strength estimations from Leeb hardness measurements. *Constr. Build. Mater.* **2020**, *261*, 119996. [CrossRef]
51. Selçuk, L.; Nar, A. Prediction of uniaxial compressive strength of intact rocks using ultrasonic pulse velocity and rebound-hammer number. *Q. J. Eng. Geol. Hydrogeol.* **2016**, *49*, 67–75. [CrossRef]
52. Yılmaz, T.; Ercikdi, B.; Karaman, K.; Külekçi, G. Assessment of strength properties of cemented paste backfill by ultrasonic pulse velocity test. *Ultrasonics* **2014**, *54*, 1386–1394. [CrossRef]
53. Kahraman, S. The correlations between the saturated and dry P-wave velocity of rocks. *Ultrasonics* **2007**, *46*, 341–348. [CrossRef]
54. Karakul, H.; Ulusay, R. Empirical correlations for predicting strength properties of rocks from P-wave velocity under different degrees of saturation. *Rock Mech. Rock Eng.* **2013**, *46*, 981–999. [CrossRef]
55. Vasanelli, E.; Sileo, M.; Calia, A.; Aiello, M.A. Non-destructive techniques to assess mechanical and physical properties of soft calcarenitic stones. *Procedia Chem.* **2013**, *8*, 35–44. [CrossRef]
56. Akoglu, K.G.; Kotoula, E.; Simon, S. Combined use of ultrasonic pulse velocity (UPV) testing and digital technologies: A model for long-term condition monitoring memorials in historic Grove Street Cemetery, New Haven. *J. Cult. Herit.* **2020**, *41*, 84–95. [CrossRef]